An efficient method to calculate the insertion loss of a rigid barrier

Weigang Wei[1], Timothy Van Renterghem[1], Dick Botteldooren[1]
[1] *Ghent University, 9000 Gent, Belgium, Email: weigang.wei@ugent.be*

Introduction

Diffraction over a rigid thick barrier can be considered as a key problem in urban sound propagation applications. A number of studies dealing with sound diffraction derived from the geometrical theory of diffraction [1][2] can be found in literature. Pierce-Hadden method [3] [4], Kouyoumjian's method [2] and Kawai's method [5] are widely used. Some recent approaches to predict sound diffraction can be found in [6][7]. Although these theoretical methods succeed in accurate predictions, they can be considered to be too complex for use in engineering models. As a result, alternative approaches focusing on efficient implementation and evaluation were developed. For example, long time ago Maekawa published an engineering model [8] to calculate the sound reduction of screens, which can not be used when the source or receiver are very close to the barrier. Salomons's approximation [9] includes multiple but suffers when the source or receiver are close to the same height with the barrier. Some more recent and widely used engineering methods, such as ISO9613-2 [10] and Harmonoise model [11][12] have drawbacks as well. The D_z part in ISO9613-2 often considerably underestimates the attenuation of a barrier compared with the long term measurement [16] and simulation; Harmonoise model overestimate the insertion loss when the barrier width is small and underestimate when the frequency is high.

In this paper, we present an efficient and accurate method to calculate the insertion loss of a rigid thick barrier by approaching the Fresnel integral with combination of triangular functions. The formulation is based on Pierce's formula [3]. First some engineering methods are introduced. Afterwards, the new method is explained in detail. Finally, the complexity, the accuracy and computational cost of different diffraction formulas are compared for some test cases. In addition, an efficient approach to include rigid ground reflections is presented.

New method to calculate A_{bar}

Overview of some commonly used methods

In this section, an overview of some widely used engineering models is listed. The details of the models can be found in relevant literature.

Pierce's diffraction method

In Pierce publication [3], the acoustic pressure at the receiver position after double diffraction is:

$$p = \frac{ie^{ikL}}{L}\left[f(Y_>) - ig(Y_>)\right]\left[f(BY_<) - ig(BY_<)\right] \quad (1)$$

$Y_>$ and $Y_<$ are the greater and smaller value of quantities Y_s and Y_r. The detailed definitions of the parameters are specified later.

ISO9613-2

In the ISO9613-2 standard, the attenuation of a barrier is described as:

$$D_z = 10\log_{10}\left[3 + (C_2/\lambda)\, C_3 z K_{met}\right] \quad (2)$$

The definition of C_2, C_3, z and K_{met} can be found in [10].

Harmonoise model

In the Harmonoise model, the Deygout's diffraction model is suggested. The description of the method can be found in [11][12].

No reflection from the ground

$A_{bar,0}$ is defined as the attenuation of a thick barrier excluding the presence of the ground. According to the literature [3, 17, 5, 18], $A_{bar,0}$ can be expressed by the following equation (3):

$$\begin{aligned} A_{bar,0} &= -10\log_{10}\left|\frac{P_{diffr}}{P_{free}}\right|^2 = -10\log_{10}\left(\left[f^2(Y_s) + g^2(Y_s)\right]\right) \\ &- 10\log_{10}\left(\left[f^2(BY_r) + g^2(BY_r)\right]\right) \end{aligned} \quad (3)$$

Definitions of parameters are shown in figure (1). Y_s and Y_r are functions of geometrical positions and diffraction angles. $Y_s = \gamma_s M_{\nu s}(\beta_s - \phi_s)$, $Y_r = \gamma_r M_{\nu r}(\beta_r - \phi_r)$, $\gamma_s = \sqrt{2r_s(w+r_r)/(\lambda L)}$, $L = \sqrt{(r_s + r_r + w)^2 + (z_s - z_r)^2}$, ($z_s = z_r$ in this model), $B = \sqrt{w(w + r_s + r_r)/\left[(w + r_s)(w + r_r)\right]}$ and $M_{\nu s}(\theta) = \frac{\cos(\nu\pi) - \cos(\nu\theta)}{\nu\sin(\nu\pi)}$. $f(Y)$ and $g(Y)$ are functions of fresnel integrals as equation (4 and 5) shown [3].

$$f(Y) = (\frac{1}{2} - S)\cos(\frac{1}{2}\pi Y^2) - (\frac{1}{2} - C)\sin(\frac{1}{2}\pi Y^2) \quad (4)$$

$$g(Y) = (\frac{1}{2} - C)\cos(\frac{1}{2}\pi Y^2) + (\frac{1}{2} - S)\sin(\frac{1}{2}\pi Y^2) \quad (5)$$

Simple form for $f^2 + g^2$ can be obtained by substituting the parameters mentioned above into equation (4 and 5).

$$f^2(Y) + g^2(Y) = C^2(Y) + S^2(Y) - C(Y) - S(Y) + 0.5 \quad (6)$$

Where Y is the input argument; C and S are Fresnel integrals:

$$C(x) = \int_0^x \cos(\frac{\pi}{2}t^2)\mathtt{d}t = \sum_{n=0}^{\infty}(-1)^n \frac{x^{4n+3}}{(2n+1)!\,(4n+3)}$$

$$S(x) = \int_0^x \sin(\frac{\pi}{2}t^2)\mathtt{d}t = \sum_{n=0}^{\infty}(-1)^n \frac{x^{4n+1}}{(2n)!\,(4n+1)}$$

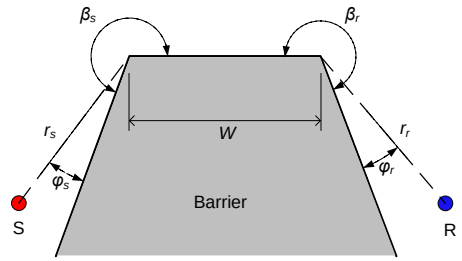

Figure 1: Parameters in a wide barrier.

For application in engineering models, calculating the Fresnel integrals is computationally demanding and difficult, so they have been approximated by trigonometric functions. In particular:

$$C(x) \approx \frac{-0.4}{x+0.4}\cos\left(1.6x^2+1.2\right)+0.5 \qquad (7)$$

$$S(x) \approx \frac{-0.4}{x+0.4}\sin\left(1.6x^2+1.2\right)+0.5 \qquad (8)$$

These two trigonometric functions fit the Fresnel integrals well when the input argument is less than 5 as shown in figure (2, 3). When the input argument is greater than 10, some phase shift can be observed. However, the quantity will fluctuate much less vigorously.

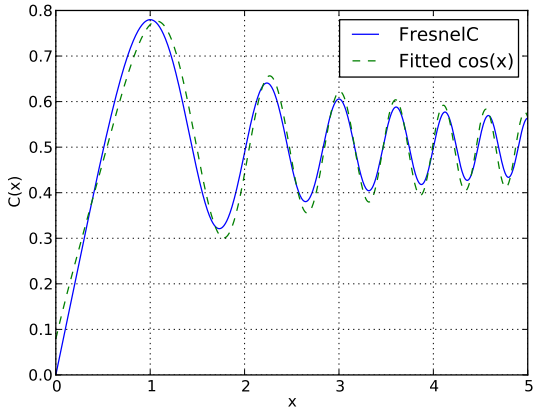

Figure 2: Theoretical value versus approximated C(x).

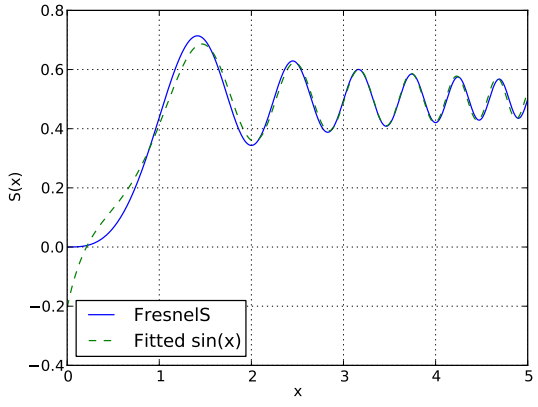

Figure 3: Theoretical value versus approximated S(x).

Equation (3) with these approximations can be further simplified to equation (9) by inserting equation (7) and (8) into equation (3).

$$A_{bar,0} \approx -10\log_{10}\left(\frac{0.4}{X_1+0.4}\right)^2\left(\frac{0.4}{X_2+0.4}\right)^2 \qquad (9)$$

Where $X_1 = Y_s$ and $X_2 = BY_r$ when $Y_s > Y_r$; $X_1 = BY_s$ and $X_2 = Y_r$ when $Y_s < Y_r$;

Reflections from the ground

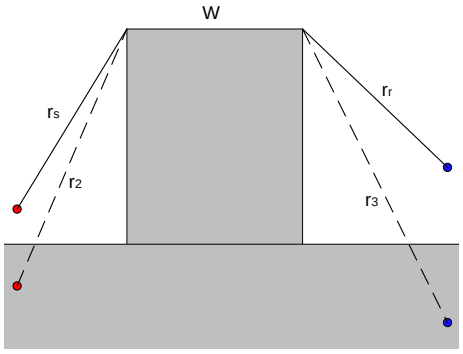

Figure 4: Sketch of thick barrier diffraction with ground.

In the previous section, the $\left|\frac{p_{diffr}}{p_{at,L}}\right|^2$ is based on excluding the presence of the ground. When a reflecting ground plane is present, the reflections would enhance the sound pressure level at the receiver position. The contributing sound path are $L_0 = r_s + W + r_r$, $L_1 = r_2 + W + r_r$, $L_2 = r_s + W + r_3$ and $L_3 = r_2 + W + r_3$ (see figure (4)). To reduce the calculation burden, a simplification is proposed to avoid calculating four times along similar sound paths. An idea is to calculate the ratio of $\left|\frac{p_{diffri}}{p_{at,Li}}\right|^2$ between different path with only path L_0. Considering equation (9), we have:

$$\frac{\left|\frac{p_{diffri}}{p_{at,Li}}\right|^2}{\left|\frac{p_{diffr0}}{p_{at,L0}}\right|^2} = \left|\frac{L_0}{L_i}\right|^2\left(\frac{Y_{0>}+0.4}{Y_{i>}+0.4}\right)^2\left(\frac{BY_{0<}+0.4}{BY_{i<}+0.4}\right)^2$$
$$= \left|\frac{L_0}{L_i}\right|^2\left(1+\frac{\Delta Y_{0i>}}{Y_{i>}+0.4}\right)^2\left(1+\frac{\Delta BY_{0i<}}{BY_{i<}+0.4}\right)^2 \qquad (10)$$

If the second order small terms are ignored, equation (10) becomes,

$$\frac{\left|\frac{p_{diffri}}{p_{at,Li}}\right|^2}{\left|\frac{p_{diffr0}}{p_{at,L0}}\right|^2} = \left|\frac{L_0}{L_i}\right|^2\left[1+2\left(\frac{\Delta Y_{0i>}}{Y_{i>}+0.4}+\frac{\Delta BY_{0i<}}{BY_{i<}+0.4}\right)\right] \qquad (11)$$

Where $\Delta Y_{0i>}$ and $\Delta Y_{0i<}$ are the difference between $Y_{0>}$, $Y_{i>}$ and $Y_{0<}$, $Y_{i<}$ respectively. $\Delta Y_{0i>}$ and $\Delta Y_{0i<}$ contain the information of the diffraction path and angle and they are supposed to be very small. In our case, the source is close to the ground, therefore, the image source could bring little differences in diffraction angle. Then we have,

$$\frac{\left|\frac{p_{diffri}}{p_{at,Li}}\right|^2}{\left|\frac{p_{diffr0}}{p_{at,L0}}\right|^2} \approx \left|\frac{L_0}{L_i}\right|^2 \qquad (12)$$

As a result, for the cases with ground reflection, the sound level referenced to free field at the receiver position (A_{bar}) can be expressed by equation (13 and 14) according to the reciprocity principle applied between image

source and receiver.

$$A_{bar,i} \approx A_{bar,0} - 10\log_{10}\left|\frac{L_0}{L_i}\right|^2 \tag{13}$$

$$A_{bar} = -10\log_{10}\sum_{i=0}^{3} 10^{-\frac{1}{10}A_{bar,i}} \tag{14}$$

Where $A_{bar,i} = -10\log_{10}\left|\frac{P_{diffr,i}}{P_{free}}\right|^2$, is the sound level relative to the free field level. L_i is the length of the diffraction path of the four combinations of source, receiver, image source, and image receiver. L_0 is the length of the diffraction path between the source and receiver.

Validation of the approximation

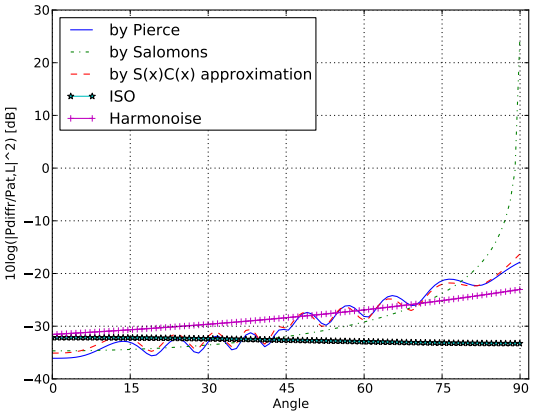

Figure 5: Comparison with the same case as reference [3] excluding the ground. Here "angle" is the angle of ϕ_r in degree.

To validate the new method, the same case as the one mentioned in reference [3] is considered. In this case $r_s = 10\lambda$, $r_r = 10\lambda$, $w = 10\lambda$, $\beta_s = \beta_r = \frac{3}{2}\pi$, $\phi_s = \pi/4$ and ϕ_r changes from 0 to $\pi/2$. Figure (5) compares the results of Pierce (indicated as "P"), Salomons (indicated as "S"), the approximation of fresnel integral as developed in the current work (indicated as "F"), "ISO" and HarmoNoise (indicated as "H"). "F" coincides very well with "P". "S" also approaches "P" accurately when the angle is small. However, when the angle approaches $\frac{\pi}{2}$, "S" tends to infinity. "ISO" does not capture the angle dependency sufficiently and gives a clear offset. "H" is also a nice approximation of "P" in this case. However, the approximation of "H" becomes worse when the wave length is shorter than 30cm, shown in figure (6). The difference between "H" and "P" is almost 10dB when $\lambda = 0.17$m and the difference will increase with the decrease of the wave length. The "F" curve becomes smoother at high frequencies but still coincides well with "P".

A full-wave numerical technique (FDTD) is used to validate the new method in case of the presence of a rigid ground plane. In this simulation, the source, whose horizontal distance to the barrier is 4.8m and vertical distance to the barrier top is 10m, is fixed 1m above the rigid ground. The receivers are 4.5m to the barrier

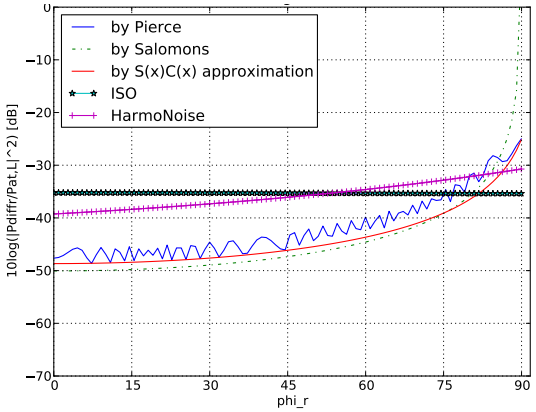

Figure 6: Comparison among different methods excluding the ground, with $\phi_s = \frac{\pi}{4}$, $\beta_s = \beta_r = \frac{3}{2}\pi$, $r_s = 10$m, $r_r = 10$m, $w = 10$m, $\lambda = 0.17$m.

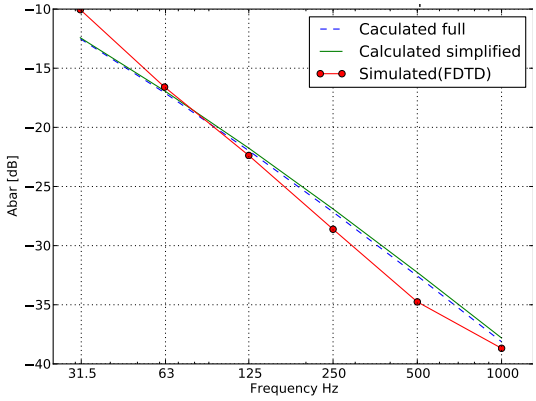

Figure 7: Comparison between full-wave technique and calculation. Receiver is 4.37m to ground. "Calculated full" indicates the insertion loss is calculated by summing up path L_0, L_1, L_2 and L_3 separately. "Calculated simplified" indicates the value is calculated by equ (13) (14).

and heights relative to the ground are 4.4m and 10.5m. Both β_s and β_r are $3\pi/2$. The width of the rigid barrier is 10m. The barrier diffraction formula coincides well with the FDTD simulation when receivers are at limited height relative to the gound plane as shown in figure (7). However, considerable offset can be observed when the receiver is at larger heights (figure 8), which is caused by the neglect of the changes in diffraction angle.

Efficiency comparison

According to the previous analysis, the new method is accurate in calculating the insertion loss of a wide rigid barrier. In this section the computational efficiency of the considered methods is discussed. Figure (9) shows the calculating speed of the four methods "S", "H", "F" and "P". "S" is the fastest method but suffers from inaccuracy. Both "S" and "F" are faster than "H" and considerably faster than "P".

Conclusion

A new method is developed based on Pierce's method to calculate the insertion loss of a rigid thick barrier. The model is validated by comparing with the analytic solution(in absence of a ground plane) and by full-wave

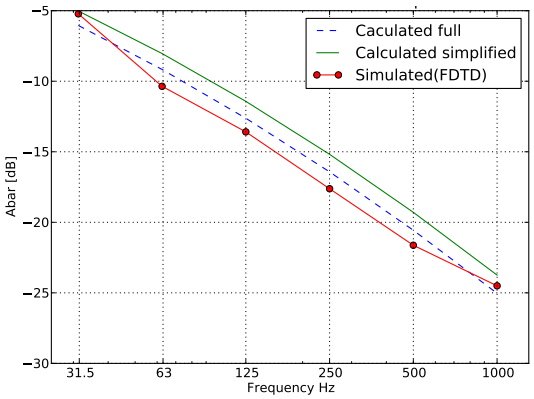

Figure 8: Comparison between full-wave technique and calculation. Receiver is 10.51m to ground.

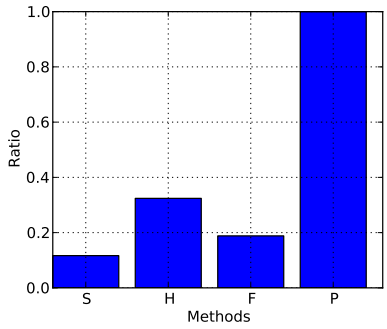

Figure 9: Comparison of calculating speed. The y-axis indicates the time ratio over methond "P"

simulations(in presence of a ground plane). The proposed method was shown to be sufficiently accurate. When ϕ_s or ϕ_r or both these angles approach to $\pi/2$, no more extreme values occur. Moreover, the calculating time is kept very limited. The model can also be generalized to multiple diffraction cases and for barriers with irregular shapes.

Acknowledge

Part of this work was financially supported by the Life+ program (project QSIDE, LIFE09 ENV/NL/000423).

References

[1] JOSEPH B. KELLER. Geometrical theory of diffraction. *Journal of the Optical Society of America*, 52(2):116–130, February 1962.

[2] R.G. Kouyoumjian and P.H. Pathak. A uniform geometrical theory of diffraction for an edge in a perfectly conducting surface. *Proceedings of the IEEE*, 62(11):1448 – 1461, November 1974.

[3] Allan D. Pierce. Diffraction of sound around corners and over wide barriers. *J. Acoust. Soc. Am.*, 55(5):941–955, 1974.

[4] Jr. W. James Hadden and Allan D. Pierce. Sound diffraction around screens and wedges for arbitrary point source locations. *The Journal of the Acoustical Society of America*, 69(5):1266–1276, 1981.

[5] T. Kawai. Sound diffraction by a many-sided barrier or pillar. *J. Sound Vib.*, 79(2):229–242, 1981.

[6] Dezhang Chu, Timothy K. Stanton, and A. D. Pierce. Higher order acoustic diffraction by edges of finite thickness. *The Journal of the Acoustical Society of America*, 122(6):3177–3194, 2007.

[7] Hequn Min and Xiaojun Qiu. Multiple acoustic diffraction around rigid parallel wide barriers. *The Journal of the Acoustical Society of America*, 126(1):179–186, 2009.

[8] Z. Maekawa. Noise reduction by screens. *Applied Acoustics*, 1(3):157–173, July 1968.

[9] Erik M. Salomons. Sound propagation in complex outdoor situations with a non-refracting atmosphere: Model based on analytical solutions for diffraction and reflection. *Acta Acust. Acust.*, 83:436–454, 1997.

[10] International Organization for Standardization. ISO 9613-2:1996 acoustics - attenuation of sound during propagation outdoors - part 2. 1996.

[11] Erik Salomons, Dirk van Maercke, Jérôme Defrance, and Foort de Roo. The harmonoise sound propagation model. *Acta Acust. Acust.*, 97(1), 2011.

[12] J. Defrance, E. Salomons, I. Noordhoek, D. Heimann, B. Plovsing, G. Watts, H. Jonasson, X. Zhang, E. Premat, I. Schmich, F. Aballea, M. Baulac, and F. de Roo. Outdoor sound propagation reference model developed in the european harmonoise project. *Acta Acust. Acust.*, 93:213–227, 2007.

[13] Danish Electronic Light & Acoustics. Nord2000. comprehensive outdoor sound propagation model. part2: Propagation in an atmosphere with refraction. Report, Danish Electronic Light & Acoustics, venlighedsvej 4, 2970 Hørsholm, Danmark, 2006.

[14] Glenn J. Wadsworth and James P. Chambers. Scale model experiments on the insertion loss of wide and double barriers. *The Journal of the Acoustical Society of America*, 107(5):2344–2350, 2000.

[15] J. Nicolas, T. F. W. Embleton, and J. E. Piercy. Precise model measurements versus theoretical prediction of barrier insertion loss in presence of the ground. *The Journal of the Acoustical Society of America*, 73(1):44–54, 1983.

[16] Timothy Van Renterghem and Dick Botteldooren. Meteorological influence on sound propagation between adjacent city canyons: A real-life experiment. *J. Acoust. Soc. Am.*, 127(6):3335-3346, 2010.

[17] Allan D. Pierce. *Acoustics: An Introduction to Its Pysical Principles and Applications*. Acoustical Society of America, New York, USA, 1989.

[18] Hyun-Sil Kim, Jae-Sueng Kim, Hyun-Ju Kang, Bong-Ki Kim, and Sang-Ryul Kim. Sound diffraction by multiple wedges and thin screens. *Applied Acoustics*, 66(9):1102–1119, September 2005.